First Observation of ^{54}Zn and its Decay by Two-Proton Emission

B. Blank,[1] A. Bey,[1] G. Canchel,[1] C. Dossat,[1] A. Fleury,[1] J. Giovinazzo,[1] I. Matea,[1] N. Adimi,[2] F. De Oliveira,[3] I. Stefan,[3]
G. Georgiev,[3] S. Grévy,[3] J. C. Thomas,[3] C. Borcea,[4] D. Cortina,[5] M. Caamano,[5] M. Stanoiu,[6] F. Aksouh,[7] B. A. Brown,[8]
F. C. Barker,[9] and W. A. Richter[10]

[1]*CENBG, Le Haut Vigneau, F-33175 Gradignan Cedex, France*
[2]*Faculté de Physique, USTHB, BP32, El Alia, 16111 Bab Ezzouar, Alger, Algeria*
[3]*Grand Accélérateur National d'Ions Lourds, B.P. 5027, F-14076 Caen Cedex, France*
[4]*Institute of Atomic Physics, P.O. Box MG6, Bucharest-Margurele, Romania*
[5]*Dpto. de Fisica de Particulas, Universidad de Santiago de Compostela, E-15782 Santiago de Compostela, Spain*
[6]*Institut de physique nucléaire d'Orsay, 15 rue Georges Clemenceau, F-91406 Orsay Cedex, France*
[7]*Instituut voor Kern- en Stralingsfysica, Celestijnenlaan 200D, B-3001 Leuven, Belgium*
[8]*Department of Physics and Astronomy and National Superconducting Cyclotron Laboratory, Michigan State University,
East Lansing, Michigan 48824-1321, USA*
[9]*Department of Theoretical Physics, Research School of Physical Sciences and Engineering, The Australian National University,
Canberra ACT 0200, Australia*
[10]*Department of Physics, University of the Western Cape, Bellville 7530, South Africa*
(Received 19 February 2005; published 13 June 2005; corrected 17 June 2005)

The nucleus ^{54}Zn has been observed for the first time in an experiment at the SISSI/LISE3 facility of
GANIL in the quasifragmentation of a ^{58}Ni beam at 74.5 MeV/nucleon in a ^{nat}Ni target. The fragments
were analyzed by means of the ALPHA-LISE3 separator and implanted in a silicon-strip detector where
correlations in space and time between implantation and subsequent decay events allowed us to generate
almost background free decay spectra for about 25 different nuclei at the same time. Eight ^{54}Zn
implantation events were observed. From the correlated decay events, the half-life of ^{54}Zn is determined
to be $3.2^{+1.8}_{-0.8}$ ms. Seven of the eight implantations are followed by two-proton emission with a decay
energy of 1.48(2) MeV. The decay energy and the partial half-life are compared to model predictions and
allow for a test of these two-proton decay models.

Our understanding of nuclear structure is mainly based on results obtained with nuclei close to the line of stability. These studies allowed for understanding of the basic structure of the strong interaction which governs the interplay between neutrons and protons in an atomic nucleus. However, these nuclei close to stability cover only a very small range in isospin; i.e., their proton-to-neutron ratio is rather similar. With the advent of machines to produce radioactive nuclei, these basic concepts can now be tested with more and more exotic nuclei having a strong imbalance of neutrons and protons.

With these exotic nuclei being much further away from stability, new phenomena also appear. For nuclei beyond the proton drip line, where the strong force can no longer bind all protons, one- and two-proton ($2p$) radioactivity was predicted more than 40 years ago by Goldanskii [1]. For odd-Z nuclei, one-proton radioactivity was proposed to occur, whereas for medium-mass and heavy-mass even-Z nuclei the nuclear pairing energy renders one-proton emission impossible. In this case, two-proton emission is to be expected.

One-proton radioactivity was observed for the first time about 20 years ago by Hofmann *et al.* [2]. Two-proton radioactivity was sought for many years without success. This research field experienced a strong boost with the advent of high-intensity projectile-fragmentation facilities. At these facilities, experimentalists could for the first time reach the most promising candidates for two-proton radioactivity. According to recent theoretical predictions, proton drip-line nuclei in the $A = 40$–55 region were identified as the most promising candidates [3–5]. The recent observation of two-proton radioactivity of ^{45}Fe [6,7] confirmed these predictions nicely. In other experiments, less promising candidates like ^{42}Cr and ^{49}Ni could be shown to decay by β-delayed processes [8]. Beyond ^{45}Fe, ^{48}Ni and ^{54}Zn were regarded as possible candidates to exhibit two-proton radioactivity. In this Letter, we report on the first observation of ^{54}Zn and its decay by two-proton radioactivity.

^{54}Zn was produced by quasifragmentation reactions of a primary ^{58}Ni^{26+} beam, accelerated to 74.5 MeV/nucleon by the GANIL cyclotrons, which impinged with an average intensity of 4 μA on a ^{nat}Ni target of thickness 250 mg/cm^2 installed in the SISSI device. The fragments were selected by the ALPHA-LISE3 separator which included a 50 μm thick beryllium degrader in the intermediate focal plane of LISE. Two micro-channel plate (MCP) detectors at the first LISE focal plane and a detection setup consisting of four silicon detectors installed at the end of the LISE3 beam line allowed us to identify the fragments

on an event-by-event basis and to study their decay properties.

The first silicon detector had a thickness of 300 μm and served to measure the energy loss (ΔE) of the fragments and their time of flight (TOF) with respect to the two MCP detectors and the radio frequency (rf) of the cyclotrons. The second silicon detector, 300 μm thick, yielded a second energy-loss signal, a TOF measurement with respect to the cyclotron rf, and served to detect β particles from the radioactive decays in the adjacent double-sided silicon-strip detector (DSSSD). The DSSSD had a thickness of 500 μm and 16 strips (3 mm-wide) on each side. It was used to measure the residual energy of the fragments and their decay characteristics. Finally, the fourth element was a 5 mm thick lithium-drifted silicon detector which served to detect β particles from radioactive decays in the DSSSD. These detectors yielded eight fragment identification parameters (two ΔE signals, two residual energies from both sides of the DSSSD, and four TOF measurements) which were used to unambiguously identify the different fragments and reject basically any background.

The experimental data were stored on tape on an event-by-event basis. To minimize the data acquisition dead time, we used two independent CAMAC/VXI branches. The trigger to start the event treatment switched from one system to the other after each event. Both branches were read out via one VME branch. In order to avoid double triggering, we increased the trigger signal width to 20 μs. This data acquisition system allowed us to treat two subsequent events as long as they are more than 20 μs apart. The event treatment lasted about 300 μs for each of the two branches, which means that we lost one event in the case where three events arrived within 300 μs. However, these events still incremented a scaler which was read out event by event. Therefore, only events which followed a preceding event within less than 20 μs got completely lost.

Figure 1 shows the fragment identification matrix for the present experiment. To generate this plot, central values and widths for the distribution of each fragment on the eight identification parameters have been determined for isotopes with a high production rate and extrapolated for the very exotic nuclei. To be accepted all eight identification parameters of an event had to lie within 3 standard deviations of the predefined values. This procedure yields basically background free identification spectra. Thus, eight events have been attributed to ^{54}Zn. This represents the first identification of this isotope. It is the most proton-rich zinc nucleus ever observed and is predicted to be particle unstable with respect to two-proton emission by all modern mass predictions. However, the Q_{2p} value varies widely (see below).

^{54}Zn has been produced by a two-proton pick-up reaction. From a production rate of about two nuclei per day, we estimate a production cross section of about $\sigma = 100$ fb.
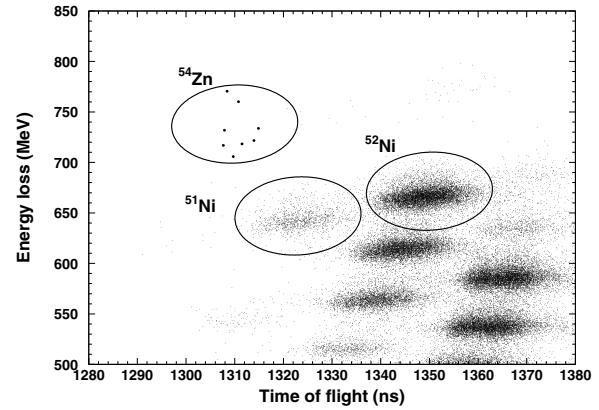

FIG. 1. Two-dimensional identification plot for the setting optimized on ^{54}Zn. Plotted is the energy loss in the first silicon detector as a function of the time of flight between one micro-channel plate detector and the first silicon detector. Eight ^{54}Zn events are identified. This figure presents only runs where a ^{54}Zn nucleus was observed.

As mentioned above, ^{54}Zn is predicted to be two-proton unbound. Figure 2 shows the decay energy spectrum measured for the first decay event in the same x-y pixel after a ^{54}Zn implantation. For eight implantations, we observe seven decay events with a decay energy of 1.48(2) MeV. None of these seven events has a coincident signal in the adjacent detectors, whereas the β-particle signals can be observed for neighboring nuclei which disintegrate by β decay. The energy calibration was performed with well-known neighboring β-delayed proton emitters and α sources. Both procedures need corrections: the β-delayed proton emitter calibration needs to be corrected for the β energy summing which was done with Monte Carlo simulations, whereas the α-particle calibration has to be corrected for the dead layer of the silicon detector. Both procedures yielded consistent results. This calibration yields the total decay energy, which includes the recoil of
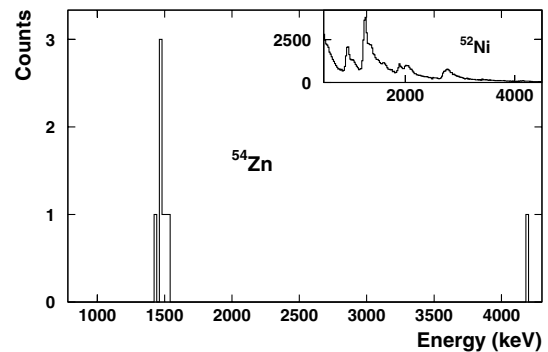

FIG. 2. Decay energy spectrum for the first decay events in the same pixel after an implantation of ^{54}Zn. A decay energy of 1.48(2) MeV is determined from the seven events in the peak. The eighth decay event has a decay energy of 4.19 MeV. The inset shows the decay energy spectrum of ^{52}Ni with the high-energy tails of the protons groups due to β pileup.

the daughter nucleus. It assumes that the pulse height defect is negligible. The total error of the decay energy is a result of the error of the energy calibration and the statistical error of the peak centroid.

The β detection efficiency for the two detectors adjacent to the DSSSD was determined by means of β-delayed proton emitters like ^{52}Ni. We determined a β efficiency of 40(5)% for the Si(Li) detector and of 20(10)% for the detector in front of the DSSSD. With these numbers, we determine a probability to miss all β particles, if ^{54}Zn would decay by a β-delayed mode with a 100% branching ratio, of $0.16^{+0.25}_{-0.15}$%. Another indication that there is no β-particle emission comes from the fact that the full width at half maximum of the ^{54}Zn peak in Fig. 2 is almost a factor of 2 narrower than, e.g., the 1.3 MeV peak from β-delayed proton emission of ^{52}Ni. This broadening for ^{52}Ni comes from the energy loss of the β particles in the DSSSD.

One decay event has an energy signal of 4.19 MeV. This event is in coincidence with a signal in the last detector identifying it as a β-delayed decay. We investigated the possibility that we missed the first decay event due to the data acquisition dead time. However, from the scaler content we found no evidence for such a loss. All events between the ^{54}Zn implantation and the subsequent decay events (^{54}Zn and daughter decays) registered by the scalers are also on tape with the complete event information. This means that the only possibility for losing the first decay event for the eighth ^{54}Zn would be if this decay happened within 20 μs of a preceding event. As the first observed decay event for this ^{54}Zn implantation happens only 1.9 ms after the implantation event which has to be compared to the half-life of ^{54}Zn (see below), we believe that it is highly likely that the 4.19 MeV event is indeed the first decay event.

From these findings, we conclude that the branching ratio for 2p emission of ^{54}Zn is BR $= 87^{+10}_{-17}$%. We will use this branching ratio to determine the partial half-life for 2p decay of ^{54}Zn which will be compared to model predictions below.

In Fig. 3, we present the decay-time distribution for the eight decay events. We determine a half-life value of $3.2^{+1.8}_{-0.8}$ ms. Together with the branching ratio for 2p emission determined above, we get a partial half-life for 2p emission of ^{54}Zn of $T^{2p}_{1/2} = 3.7^{+2.2}_{-1.0}$ ms.

Another indication for the occurrence of 2p radioactivity is the observation of the decay of the 2p daughter, ^{52}Ni. This nucleus decays by β-delayed proton emission with proton energies of 1.06 and 1.34 MeV and branching ratios of 4% and 10%, respectively [9]. We observe indeed 2 second decay events with energies in agreement with these expectations. However, ^{52}Ni decays by β-delayed γ emission with a branching ratio of 70%. In these cases, we have a probability of only about 15% to detect the β particle in the DSSSD and therefore to be able to correlate it properly with the ^{54}Zn implantation.
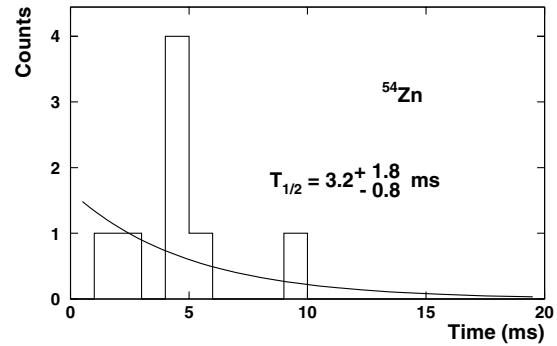

FIG. 3.   The half-life of ^{54}Zn is determined by means of the decay-time distribution of the first decay events after ^{54}Zn implantation. The half-life determined is given in the figure.

The experimental information collected above can only be explained consistently by the assumption of a decay by two-proton radioactivity of ^{54}Zn with a branching ratio of 87^{+10}_{-17}%. All other possible decay modes do not yield a consistent picture. For β-delayed decays, we would expect to observe for a few decays the β particle as well as a broadening of the peak. For α radioactivity, the barrier-penetration half-life for an α particle with an energy of 1.48 MeV is several minutes, while the same barrier penetration lasts only about 10^{-17} s in the case of one-proton emission with a decay energy of 1.48 MeV. We therefore conclude that we have observed ground-state two-proton radioactivity for ^{54}Zn. In the following paragraphs, we will compare the experimental partial half-life of $T^{2p}_{1/2} = 3.7^{+2.2}_{-1.0}$ ms and the 2p decay energy of $E_{2p} = 1.48(2)$ MeV to different model predictions.

Starting from the 2p decay energy, we can determine the mass excess of ^{54}Zn. Using the mass excess of ^{52}Ni as determined by means of the isobaric multiplet mass equation of $\Delta m = -22.64(4)$ MeV [9], we obtain a mass excess of $\Delta m = -6.58(4)$ MeV for ^{54}Zn. This mass excess compares well with, e.g., the mass prediction of -6.34 MeV from Jänecke and Masson [10] and the mass extrapolation of $-6.57(40)$ MeV from Audi and co-workers [11].

The decay energy E_{2p} was recently predicted by several authors. Brown *et al.* [3] proposed an energy of 1.33(14) MeV. Ormand [4] determined an energy of 1.97(24) MeV, whereas Cole [5] predicted a value of 1.79(12) MeV. All these theoretical decay energies are reasonably close to our experimental datum. However, when used in a simple barrier-penetration di-proton model, which is expected to yield only a lower limit for the partial half-life for 2p decay [12], we obtain values between 20 ms and 10^{-17} ms, a rather large spread.

Such a di-proton model completely neglects any nuclear structure or any dynamics of the decay. Grigorenko and co-workers [12,13] developed a model which explicitly includes the decay dynamics by modelling the proton-proton and proton-core interaction in the decay. Their three-body
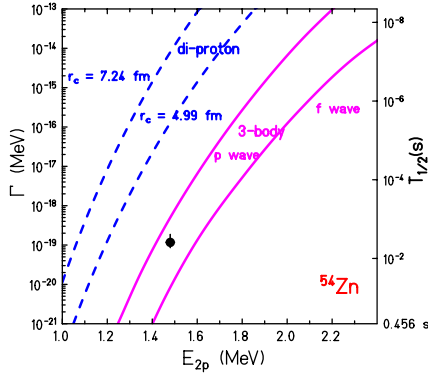
FIG. 4 (color online).   Relation between half-life/decay width and decay energy as determined by the three-body model of Grigorenko *et al.* [13]. The picture compares the experimental datum to the three-body model (solid lines) with two different assumptions for the proton emitting orbital and with the di-proton model (dashed lines) for two different channel radii.

model result is compared to our experimental result in Fig. 4. We obtain reasonable agreement between experiment and theory, if we assume that the two protons are emitted from a p orbital, as expected from simple shell-model arguments. The three-body model yields much longer half-lives for a given decay energy than the simple di-proton model.

The three-body model contains only little nuclear structure information, but treats the dynamics in a reasonable fashion. Brown and Barker developed the R-matrix approach to apply it for $2p$ emission [14,15]. This model includes the s-wave proton-proton interaction as an intermediate state. The nuclear structure input is the spectroscopic factor [16] $S = (\frac{A}{A-2})^{\lambda} G^2(pf) C(A, Z)$ where $G^2 = 5/16$, $\lambda = 6$, A is the mass of the parent nucleus ($A = 54$), and $C(A, Z) = |\langle \Psi(A-2, Z-2) | \psi_c | \Psi(A, Z) \rangle|^2$ is the cluster overlap for the di-proton cluster wave function ψ_c in the pf shell with $L = 0$, $S = 0$, and $T = 1$ in the SU3 basis. The pf-shell wave functions Ψ were obtained with the recent GPFX1 interaction [17] with the result $C = 0.63$. For the di-proton-nucleus potential, we take a Woods-Saxon form plus a uniform-sphere Coulomb potential with radius $R_C = r_C A^{1/3}$. The Woods-Saxon parameters are $R = r_0 A^{1/3}$ for the radius, a_0 for the diffuseness, and a well depth adjusted to reproduce the resonance energy. The potential parameters are taken from an analysis of low-energy deuteron scattering [18]: $r_0 = 1.17$ fm, $a_0 = 0.72$ fm, and $r_C = 1.30$ fm. These are the same potential parameters used for the calculation of the di-proton decay for ^{45}Fe in Ref. [15].

With the experimental Q value of 1.48(2) MeV, the resulting half-life is 10^{+7}_{-4} ms, whereas the value is 6^{+3}_{-2} μs when the p-p resonance is ignored. The experimental decay rate is 1–6 times faster than the theoretical value which takes into account the p-p resonance. A similar enhancement was found in the comparison of ex-

periment and theory for ^{45}Fe [15]. Pairing correlations due to configuration mixing beyond the pf shell may account for this enhancement. In Ref. [19], an enhancement factor of about two (the ratio of the ϵ factors in columns 3 and 5 of Table 3 of that paper) due to mixing with the sd and $g_{9/2}$ orbitals was calculated for the two-neutron transfer in the (p, t) reaction in the pf shell. Calculations of the two-proton decay that include orbitals outside the pf shell remain to be carried out.

In summary, we observed for the first time the new isotope ^{54}Zn. As predicted by modern mass models, it decays by two-proton emission with a decay energy of $E_{2p} = 1.48(2)$ MeV. The two-proton branching ratio is $87^{+10}_{-17}\%$ and the total half-life was determined to be $3.2^{+1.8}_{-0.8}$ ms yielding a $2p$ partial half-life of $T^{2p}_{1/2} = 3.7^{+2.2}_{-1.0}$ ms. The two advanced models able to describe two-proton radioactivity achieve reasonable agreement with our experimental data. Future studies will try to find more cases of two-proton radioactivity and investigate the decay in more detail by measuring the p-p angular correlation and the energy of the individual protons.

[1] V. I. Goldanskii, Nucl. Phys. **19**, 482 (1960).
[2] S. Hofmann *et al.*, Z. Phys. A **305**, 111 (1982).
[3] B. A. Brown *et al.*, Phys. Rev. C **65**, 045802 (2002).
[4] W. E. Ormand, Phys. Rev. C **55**, 2407 (1997).
[5] B. J. Cole, Phys. Rev. C **54**, 1240 (1996).
[6] J. Giovinazzo *et al.*, Phys. Rev. Lett. **89**, 102501 (2002).
[7] M. Pfützner *et al.*, Eur. Phys. J. A **14**, 279 (2002).
[8] J. Giovinazzo *et al.*, Eur. Phys. J. A **10**, 73 (2001).
[9] C. Dossat, Ph.D. thesis, University Bordeaux I, 2004 (unpublished).
[10] J. Jänecke and P. Masson, At. Data Nucl. Data Tables **39**, 265 (1988).
[11] G. Audi, O. Bersillon, J. Blachot, and A. H. Wapstra, Nucl. Phys. **A729**, 3 (2003).
[12] L. Grigorenko *et al.*, Phys. Rev. C **64**, 054002 (2001).
[13] L. Grigorenko and M. Zhukov, Phys. Rev. C **68**, 054005 (2003).
[14] F. C. Barker, Phys. Rev. C **63**, 047303 (2001).
[15] B. A. Brown and F. C. Barker, Phys. Rev. C **67**, 041304 (2003).
[16] N. Anyas-Weiss *et al.*, Phys. Rep. **12**, 201 (1974).
[17] M. Honma, T. Otsuka, B. A. Brown, and T. Mizusaki, Phys. Rev. C **69**, 034335 (2004).
[18] W. W. Daehnick, J. D. Childs, and Z. Vrcelj, Phys. Rev. C **21**, 2253 (1980).
[19] P. Decowski, W. Benenson, B. A. Brown, and H. Nann, Nucl. Phys. **A302**, 186 (1978).